

Entanglement Classification of Restricted Greenberger-Horne-Zeilinger Symmetric States in Four-Qubit System

DaeKil Park^{1,2}

¹*Department of Physics, Kyungnam University, Changwon 631-701, Korea*

²*Department of Electronic Engineering,
Kyungnam University, Changwon 631-701, Korea*

Abstract

Similar to the three-qubit Greenberger-Horne-Zeilinger (GHZ) symmetry we explore the four-qubit GHZ symmetry group and its subgroup called restricted GHZ symmetry group. While the set of symmetric states under the whole group transformation is represented by three real parameters, the set of symmetric states under the subgroup transformation is represented by two real parameters. After comparing the symmetric states for whole and subgroup, the entanglement is examined for the latter set. It is shown that the set has only two SLOCC classes, L_{abc_2} and G_{abcd} . Extension to the multi-qubit system is briefly discussed.

I. INTRODUCTION

Quantum entanglement[1] is the most important notion in quantum technology (QT) and quantum information theory (QIT). As shown for last two decades it plays a crucial role in quantum teleportation[2], superdense coding[3], quantum cloning[4], and quantum cryptography[5]. It is also quantum entanglement, which makes the quantum computer outperform the classical one[6, 7]. Thus, in order to develop QT and QIT it is essential to understand how to quantify and how to characterize the multipartite entanglement.

The most plausible scheme for the entanglement classification is characterization through local unitary (LU) transformation. If $|\psi\rangle$ and $|\varphi\rangle$ are in the same category in LU, one state can be obtained with certainty from the other one by means of local operations assisted classical communication (LOCC)[8, 9]. This implies that $|\psi\rangle$ and $|\varphi\rangle$ can be used, respectively, to implement the same task of QIT with equal probability of successful performance of the task. However, the classification through LU generates infinite equivalence classes even in the simplest bipartite systems.

In order to escape this difficulty the classification through stochastic local operations and classical communication (SLOCC) was introduced in Ref.[8]. If $|\psi\rangle$ and $|\varphi\rangle$ are in the same SLOCC class, one state can be converted into the other state with nonzero probability by means of LOCC. This fact implies that $|\psi\rangle$ and $|\varphi\rangle$ can be used, respectively, to implement the same task of QIT although the probability of success for this task is different. Mathematically, if two n -party states $|\psi\rangle$ and $|\varphi\rangle$ are in the same SLOCC class, they are related to each other by $|\psi\rangle = A_1 \otimes A_2 \otimes \dots \otimes A_n |\varphi\rangle$ with $\{A_j\}$ being arbitrary invertible local operators¹. However, it is more useful to restrict ourselves to SLOCC transformation where all $\{A_j\}$ belong to $SL(2, C)$, the group of 2×2 complex matrices having determinant equal to 1.

The SLOCC classification was first examined in the three-qubit pure-state system[10]. It was shown that the whole system consists of six inequivalent SLOCC classes, i.e., fully separable (S), three bi-separable (B), W, and Greenberger-Horne-Zeilinger (GHZ) classes. Moreover, it is possible to know which class an arbitrary state $|\psi\rangle$ belongs by computing the residual entanglement[11] and concurrences[12] for its partially reduced states. Similarly,

¹ For complete proof on the connection between SLOCC and local operations see Appendix A of Ref.[10].

the entanglement of whole three-qubit mixed states consists of S, B, W, and GHZ types[13]. It was shown that these classes satisfy a linear hierarchy $S \subset B \subset W \subset \text{GHZ}$.

Generally, a given QIT task requires a particular type of entanglement. In addition, the effect of environment generally converts the pure state prepared for the QIT task into the mixed state. Therefore, it is important to distinguish the entanglement of mixtures to perform the QIT take successfully. However, it is notoriously difficult problem to know which type of entanglement is contained in the given multipartite mixed state. Even for three-qubit state it is very difficult problem because analytical computation of the residual entanglement for arbitrary mixed states is generally impossible so far².

Recently, classification of the entanglement classes for three-qubit mixed states has been significantly progressed. In Ref.[15] the GHZ symmetry was examined in three-qubit system. This symmetry is a symmetry that GHZ states $|\text{GHZ}_3\rangle_{\pm} = (1/\sqrt{2})(|000\rangle \pm |111\rangle)$ have up to the global phase and is expressed as a symmetry under (i) qubit permutation, (ii) simultaneous flips, (iii) qubit rotation about the z -axis. The whole GHZ-symmetric states can be parametrized by two real parameters, *say* x and y . Authors in Ref. [15] succeeded in classifying the entanglement of the GHZ-symmetric states completely. This complete classification makes it possible to compute the three-tangle³ analytically for the GHZ-symmetric states[16] and to construct the class-specific optimal witnesses[17]. It also makes it possible to obtain lower bound of three-tangle for arbitrary 3-qubit mixed state[18]. More recently, The SLOCC classification of the extended GHZ-symmetric states was discussed[19]. Extended GHZ symmetry is the GHZ symmetry without qubit permutation symmetry. It is larger symmetry group than usual GHZ symmetry group, and is parametrized by four real parameters.

The purpose of this paper is to extend the analysis of Ref.[15] to four-qubit system. Four-qubit GHZ states⁴ (or 4-cat states[8], in honor of Schrödinger's cat) are defined as

$$|\text{GHZ}_4\rangle_{\pm} = \frac{1}{\sqrt{2}}(|0000\rangle \pm |1111\rangle). \quad (1.1)$$

² However, it is possible to compute the residual entanglement for few rare cases[14].

³ The definition of three-tangle in this paper is a square root of the residual entanglement presented in Ref.[11].

⁴ While $|\text{GHZ}_3\rangle_+$ is an unique maximally entangled 3-qubit state up to LU, $|\text{GHZ}_4\rangle_+$ is not unique maximally entangled state. In 4-qubit system there are two more additional maximally entangled states $|\Phi_5\rangle = (1/\sqrt{6})(\sqrt{2}|1111\rangle + |1000\rangle + |0100\rangle + |0010\rangle + |0001\rangle)$ and $|\Phi_4\rangle = (1/2)(|1111\rangle + |1100\rangle + |0010\rangle + |0001\rangle)$ [20].

Like a 3-qubit GHZ symmetry we define a 4-qubit GHZ symmetry as a symmetry which $|\text{GHZ}_4\rangle_{\pm}$ have up to the global phase. Straightforward generalization, which is (i) qubit permutation, (ii) simultaneous flips, (iii) qubit rotation about the z -axis of the form

$$U(\phi_1, \phi_2, \phi_3) = e^{i\phi_1\sigma_z} \otimes e^{i\phi_2\sigma_z} \otimes e^{i\phi_3\sigma_z} \otimes e^{-i(\phi_1+\phi_2+\phi_3)\sigma_z}, \quad (1.2)$$

is obviously a symmetry of $|\text{GHZ}_4\rangle_{\pm}$. Thus, we will call this symmetry as 4-qubit GHZ symmetry. As will be shown later the 4-qubit GHZ-symmetric states are represented by three real parameters while 3-qubit states contain only two. Thus, it is more difficult to analyze the entanglement classification in 4-qubit GHZ-symmetric case than that in 3-qubit case. Since this is first extension of Ref.[15] to the 4-qubit system, we would like to consider more simple case by reducing the number of parameters. This can be achieved by modifying (ii) into (ii) simultaneous and any pair flips without changing (i) and (iii). The simplest state which has the modified symmetry (ii) is

$$|\psi\rangle_{ABCD} = \frac{1}{2\sqrt{2}}(|0000\rangle + |1100\rangle + |1010\rangle + |1001\rangle + |0110\rangle + |0101\rangle + |0011\rangle + |1111\rangle). \quad (1.3)$$

It is easy to show that $|\psi\rangle_{ABCD}$ is symmetric under the flips of (A, B) , (A, C) , (A, D) , (B, C) , (B, D) , (C, D) , or (A, B, C, D) parties. Therefore, $|\text{GHZ}_4\rangle_{\pm}$ do not have this modified symmetry obviously. Of course, the states, which have this modified symmetry, are also GHZ-symmetric. Therefore, we call this modified symmetry as restricted GHZ (RGHZ) symmetry⁵. As will be shown, the RGHZ-symmetric states is represented by two real parameters like the 3-qubit case.

This paper is organized as follows. In section II the general forms of the GHZ- and RGHZ-symmetric states are derived, respectively. It is shown that while the GHZ-symmetric states are represented by three real parameters, the RGHZ-symmetric states are represented by two real parameters. In section III we classify the entanglement of the RGHZ-symmetric states. It is shown that entanglement of the RGHZ-symmetric states is either L_{abc_2} or G_{abcd} . In section IV a brief conclusion is given.

⁵ The state $|\psi\rangle_{ABCD}$ given in Eq. (1.3) is not RGHZ-symmetric because it is not symmetric under the qubit rotation about the z -axis although it is symmetric under the modified (ii). In fact, there is no pure RGHZ-symmetric state.

II. GHZ-SYMMETRIC AND RGHZ-SYMMETRIC STATES

In this section we will derive the general forms of the GHZ-symmetric and RGHZ-symmetric states and compare them with each other.

A. GHZ-symmetric states

It is not difficult to show that the general form of the GHZ-symmetric states is

$$\begin{aligned} \rho_4^{\text{GHZ}} = & \tilde{x} [|0000\rangle\langle 1111| + |1111\rangle\langle 0000|] \\ & + \text{diag}(\tilde{\alpha}_1, \tilde{\alpha}_2, \tilde{\alpha}_2, \tilde{\alpha}_3, \tilde{\alpha}_2, \tilde{\alpha}_3, \tilde{\alpha}_3, \tilde{\alpha}_2, \tilde{\alpha}_3, \tilde{\alpha}_2, \tilde{\alpha}_3, \tilde{\alpha}_2, \tilde{\alpha}_3) \end{aligned} \quad (2.1)$$

where \tilde{x} , $\tilde{\alpha}_1$, $\tilde{\alpha}_2$ and $\tilde{\alpha}_3$ are real numbers satisfying $\tilde{\alpha}_1 + 4\tilde{\alpha}_2 + 3\tilde{\alpha}_3 = \frac{1}{2}$. Unlike the three-qubit case, ρ_4^{GHZ} is represented by three real parameters.

Now, we define following two real parameters \tilde{y} , \tilde{z} , as

$$\begin{aligned} \tilde{y} &= \mathcal{N}_1 \left[\tilde{\alpha}_1 + (\sqrt{10} + 3)\tilde{\alpha}_2 \right] \\ \tilde{z} &= \mathcal{N}_2 \left[(\sqrt{10} + 3)\tilde{\alpha}_1 - \tilde{\alpha}_2 \right] \end{aligned} \quad (2.2)$$

where

$$\mathcal{N}_1 = \sqrt{\frac{2}{3} - \frac{2}{15}\sqrt{10}} \approx 0.495 \quad \mathcal{N}_2 = \sqrt{\frac{14}{3} - \frac{22}{15}\sqrt{10}} \approx 0.169. \quad (2.3)$$

Then, it is straightforward to show that the Hilbert-Schmidt metric of ρ_4^{GHZ} is equal to the Euclidean metric, i.e.,

$$d^2 \left[\rho_4^{\text{GHZ}}(\tilde{\alpha}_1, \tilde{\alpha}_2, \tilde{\alpha}_3, \tilde{x}), \rho_4^{\text{GHZ}}(\tilde{\alpha}'_1, \tilde{\alpha}'_2, \tilde{\alpha}'_3, \tilde{x}') \right] = (x - x')^2 + (y - y')^2 + (z - z')^2 \quad (2.4)$$

where $d^2(A, B) = \frac{1}{2}\text{tr}(A - B)^\dagger(A - B)$.

In order for ρ_4^{GHZ} to be a physical state we have the restrictions

$$0 \leq \tilde{\alpha}_2 \leq \frac{1}{8} \quad 0 \leq \tilde{\alpha}_3 \leq \frac{1}{6} \quad 0 \leq \tilde{\alpha}_1 \leq \frac{1}{2} \quad (2.5)$$

and

$$\tilde{\alpha}_1 \geq \pm\tilde{x}. \quad (2.6)$$

This physical conditions imply that any GHZ-symmetric physical state is represented as a point inside a tetrahedron shown in Fig. 1(a). In this figure two black dots represent $|\text{GHZ}_4\rangle_{\pm}$, respectively. It is worthwhile noting that the sign of x does not change the character of entanglement because $\rho_4^{\text{GHZ}}(-\tilde{x}, \tilde{y}, \tilde{z}) = u\rho_4^{\text{GHZ}}(\tilde{x}, \tilde{y}, \tilde{z})u^\dagger$, where $u = i\sigma_x \otimes \sigma_y \otimes \sigma_y \otimes \sigma_y$.

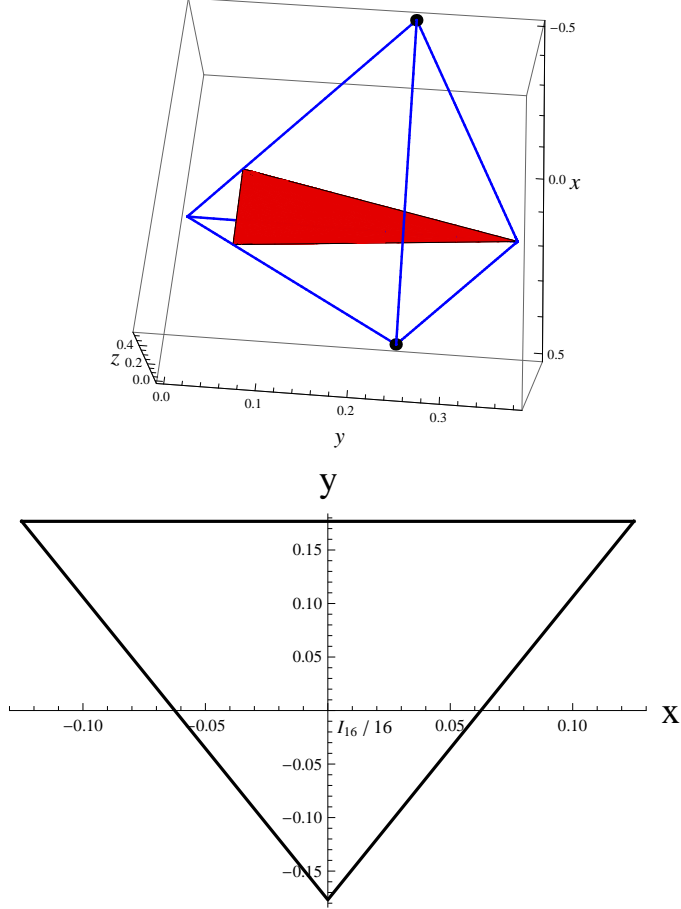


FIG. 1: (Color online) Each point in tetrahedron is correspondent to the GHZ-symmetric state. Two black dots represent the 4-qubit GHZ state $|\text{GHZ}_4\rangle_{\pm}$. The surface of triangle in the tetrahedron is the place where the RGHZ-symmetric states reside. (b) Each point in triangle is correspondent to the RGHZ-symmetric state. This triangle is equivalent to the triangle in Fig. 1(a). Thus, RGHZ symmetric states have very small portion and are of zero measure in the whole set of the GHZ-symmetric states.

B. RGHZ-symmetric states

It is straightforward to show that the general form of RGHZ-symmetric states is

$$\rho_4^{\text{RGHZ}} = x [|0000\rangle\langle 1111| + |1111\rangle\langle 0000|] \quad (2.7)$$

$$+ \text{diag}(\alpha_1, \alpha_2, \alpha_2, \alpha_1, \alpha_2, \alpha_1, \alpha_1, \alpha_2, \alpha_2, \alpha_1, \alpha_1, \alpha_2, \alpha_2, \alpha_1, \alpha_2, \alpha_2, \alpha_1)$$

with $\alpha_1 = \frac{1}{16} + \frac{y}{2\sqrt{2}}$ and $\alpha_2 = \frac{1}{16} - \frac{y}{2\sqrt{2}}$. The parameters x and y are chosen such that the Euclidean metric in the (x, y) plane coincides with the Hilbert-Schmidt metric $d^2(A, B) =$

$\frac{1}{2}\text{tr}(A - B)^\dagger(A - B)$ again. It is also worthwhile noting that the sign of x does not change the entanglement because $\rho_4^{\text{RGHZ}}(-x, y) = u\rho_4^{\text{RGHZ}}(x, y)u^\dagger$. This is evident from the fact that the RGHZ-symmetric state is also GHZ-symmetric.

Since ρ_4^{RGHZ} is a quantum state, it should be a positive operator, which restricts the parameters as

$$y \geq \pm 2\sqrt{2}x - \frac{\sqrt{2}}{8} \quad |x| \leq \frac{1}{8}. \quad (2.8)$$

Thus any RGHZ-symmetric physical state is represented as a point in a triangle depicted in Fig. 1(b).

It is easy to show that ρ_4^{GHZ} is RGHZ-symmetric if and only if $\tilde{x} = x$, $\tilde{\alpha}_2 = \alpha_2$, and $\tilde{\alpha}_1 = \tilde{\alpha}_3 = \alpha_1$ or equivalently

$$\tilde{y} = \mathcal{N}_1 \left[\frac{\sqrt{10} + 4}{16} - \frac{\sqrt{10} + 2}{2\sqrt{2}}y \right] \quad \tilde{z} = \mathcal{N}_2 \left[\frac{\sqrt{10} + 2}{16} - \frac{\sqrt{10} + 4}{2\sqrt{2}}y \right]. \quad (2.9)$$

Using this relation it is possible to know where the RGHZ-symmetric states reside in the tetrahedron in Fig. 1(a). In this figure the red triangle is equivalent one of Fig. 1(b). Thus, the states on this triangle are RGHZ-symmetric. From Fig. 1(a) one can realize that the RGHZ-symmetric states have very small portion and are of zero measure in the entire set of GHZ-symmetric states.

III. SLOCC CLASSIFICATION OF RGHZ-SYMMETRIC STATES

The SLOCC classification of the 4-qubit pure-state system was first discussed in [21] by making use of the Jordan block structure of some complex symmetric matrix. Subsequently, same issue was explored in several more papers using different approaches[22]. Unlike, however, two- and three-qubit cases, the results of Ref.[21, 22] seem to be contradictory to each other. This means that still our understanding on the 4-qubit entanglement is incomplete.

In this paper we adopt the results of [21], where there are following nine inequivalent

SLOCC classes;

$$\begin{aligned}
G_{abcd} &= \frac{a+d}{2}(|0000\rangle + |1111\rangle) + \frac{a-d}{2}(|0011\rangle + |1100\rangle) \\
&\quad + \frac{b+c}{2}(|0101\rangle + |1010\rangle) + \frac{b-c}{2}(|0110\rangle + |1001\rangle) \\
L_{abc_2} &= \frac{a+b}{2}(|0000\rangle + |1111\rangle) + \frac{a-b}{2}(|0011\rangle + |1100\rangle) \\
&\quad + c(|0101\rangle + |1010\rangle) + |0110\rangle \\
L_{a_2b_2} &= a(|0000\rangle + |1111\rangle) + b(|0101\rangle + |1010\rangle) + |0110\rangle + |0011\rangle \\
L_{ab_3} &= a(|0000\rangle + |1111\rangle) + \frac{a+b}{2}(|0101\rangle + |1010\rangle) \\
&\quad + \frac{a-b}{2}(|0110\rangle + |1001\rangle) + \frac{i}{\sqrt{2}}(|0001\rangle + |0010\rangle + |0111\rangle + |1011\rangle) \\
L_{a_4} &= a(|0000\rangle + |0101\rangle + |1010\rangle + |1111\rangle) + (i|0001\rangle + |0110\rangle - i|1011\rangle) \\
L_{a_2 0_{3\oplus\bar{1}}} &= a(|0000\rangle + |1111\rangle) + (|0011\rangle + |0101\rangle + |0110\rangle) \\
L_{0_{5\oplus\bar{3}}} &= |0000\rangle + |0101\rangle + |1000\rangle + |1110\rangle \\
L_{0_{7\oplus\bar{1}}} &= |0000\rangle + |1011\rangle + |1101\rangle + |1110\rangle \\
L_{0_{3\oplus\bar{1}} 0_{3\oplus\bar{1}}} &= |0000\rangle + |0111\rangle,
\end{aligned} \tag{3.1}$$

where a , b , c , and d are complex parameters with nonnegative real part. In Eq. (3.1) G_{abcd} is special in a sense that its all local states are completely mixed. In other words, G_{abcd} is a set of normal states[23].

A. L_{abc_2}

In this subsection we examine a question where the states of L_{abc_2} reside in the triangle in Fig. 1(b). Before proceeding further, it is important to note that there is a correspondence between four-qubit pure states and RGHZ-symmetric states. Let $|\psi\rangle$ be a four-qubit pure state. Then, the corresponding RGHZ-symmetric state $\rho_4^{\text{RGHZ}}(\psi)$ can be written as

$$\rho_4^{\text{RGHZ}}(\psi) = \int U|\psi\rangle\langle\psi|U^\dagger, \tag{3.2}$$

where the integral is understood to cover the entire RGHZ symmetry group, i.e., unitaries $U(\phi_1, \phi_2, \phi_3)$ in Eq. (1.2) and averaging over the discrete symmetries. For example, if

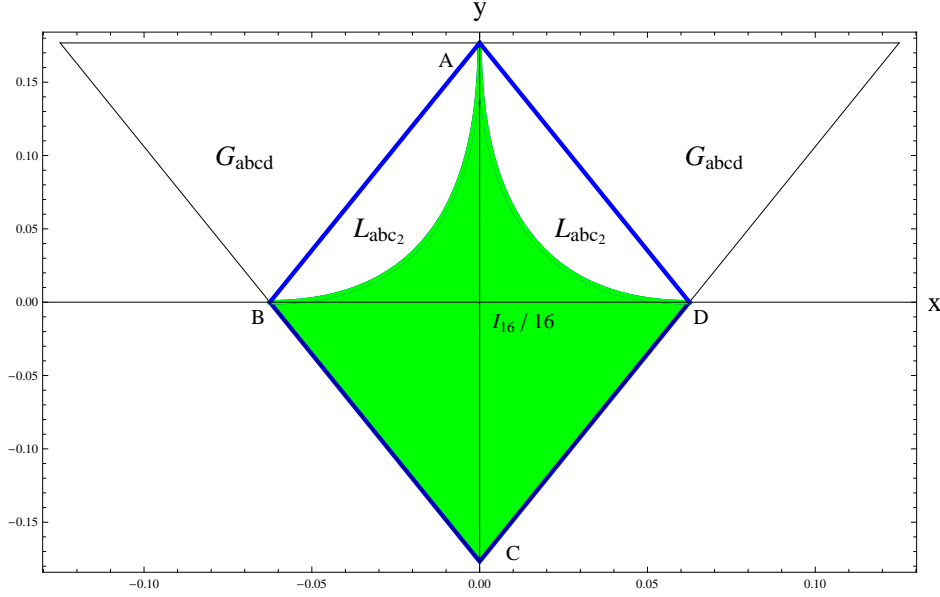


FIG. 2: (Color online) The SLOCC classification of RGHZ-symmetric states ρ_4^{RGHZ} . In the polygon ABCD states of L_{abc_2} reside. Theorem 2 implies that there is no one-qubit tensor product three-qubit entangled states in the GHZL-symmetric states. This fact implies that the RGHZ symmetry exclude $L_{a_2 0_{3\oplus\bar{1}}}$, $L_{0_{3\oplus\bar{1}} 0_{3\oplus\bar{1}}}$, and $L_{a_2 b_2}$. Theorem 3 implies that there are states of G_{abcd} outside of the polygon ABCD.

$|\psi\rangle = \sum_{i,j,k,l=0}^1 \psi_{ijkl} |ijkl\rangle$, $\rho_4^{\text{RGHZ}}(\psi)$ becomes Eq. (2.7) with

$$\begin{aligned}
 x &= \frac{1}{4} \text{Re} \left[\psi_{0000} \psi_{1111}^* + \psi_{0011} \psi_{1100}^* + \psi_{0101} \psi_{1010}^* + \psi_{0110} \psi_{1001}^* \right] \\
 \alpha_1 &\equiv \frac{1}{16} + \frac{y}{2\sqrt{2}} = \frac{1}{8} \left[|\psi_{0000}|^2 + |\psi_{1111}|^2 + |\psi_{0011}|^2 + |\psi_{0101}|^2 \right. \\
 &\quad \left. + |\psi_{0110}|^2 + |\psi_{1001}|^2 + |\psi_{1010}|^2 + |\psi_{1100}|^2 \right].
 \end{aligned} \tag{3.3}$$

Now, we are ready to discuss the main issue of this subsection.

Theorem 1. *The RGHZ-symmetric states of L_{abc_2} -class reside in the polygon ABCD in Fig. 2.*

Proof. First we note that when $a = b = c = 0$, L_{abc_2} reduces to the fully separable state $|0110\rangle$. Since LU is a particular case of SLOCC, this fact implies that all fully separable

states are in the L_{abc_2} . Let $|\psi^{sep}\rangle = (u_1 \otimes u_2 \otimes u_3 \otimes u_4)|0000\rangle$, where

$$u_j = \begin{pmatrix} A_j & -C_j^* \\ C_j & A_j^* \end{pmatrix} \quad \text{with } |A_j|^2 + |C_j|^2 = 1. \quad (3.4)$$

Then, it is easy to derive the parameters x and y of $\rho_4^{\text{RGHZ}}(\psi^{sep})$ easily using Eq. (3.3). Our method for proof is as follows. Applying the Lagrange multiplier method we maximize x with given y . Then, it is possible to derive a boundary $x_{\max} = x_{\max}(y)$ in the (x, y) plane. If a region inside the boundary is convex, this is the region where the L_{abc_2} -class states reside. If it is not convex, we have to choose the convex hull of it for the residential region.

From the symmetry it is evident that the maximum of x occurs when $A_1 = A_2 = A_3 = A_4 \equiv A$, Then the constraint of y yields $A^2 = \frac{1}{2} (1 \pm 2^{5/8} y^{1/4})$, which gives

$$x_{max} = \frac{1}{16} \left(1 - 2^{\frac{5}{4}} y^{\frac{1}{2}} \right)^2. \quad (3.5)$$

Since the sign of x_{max} does not change the entanglement class, the region represented by green color in Fig. 2 is derived. Since it is not convex, we have to choose a convex hull, which is a polygon ABCD in Fig. 2. This completes the proof.

Although we start with fully separable state, this does not guarantee that all states in the polygon ABCD are fully separable because L_{abc_2} has 4-way entangled states as well as fully separable states. The only fact we can assert is that all L_{abc_2} -class RGHZ-symmetric states reside in the polygon ABCD.

B. $L_{a_2 0_{3\oplus 1}}, L_{0_{3\oplus 1} 0_{3\oplus 1}}, \dots$

In this subsection we will show that the RGHZ symmetry excludes all SLOCC classes except G_{abcd} .

Theorem 2. *There is no one-qubit product GHZ state in the RGHZ-symmetric states.*

Proof. Let $|\psi^{GHZ}\rangle = (G_1 \otimes G_2 \otimes G_3 \otimes G_4)|0\rangle \otimes (|000\rangle + |111\rangle)$, where

$$G_j = \begin{pmatrix} A_j & B_j \\ C_j & D_j \end{pmatrix}. \quad (3.6)$$

Then, it is easy to compute x and y of $\rho_4^{\text{RGHZ}}(\psi^{GHZ})$ using Eq. (3.3). Now, we want to maximize x with given y and $\langle \psi^{GHZ} | \psi^{GHZ} \rangle = 1$. From symmetry of the Lagrange multiplier

equations it is evident that the maximum of x occurs when $A_2 = A_3 = A_4 = B_2 = B_3 = B_4 \equiv a$ and $C_2 = C_3 = C_4 = D_2 = D_3 = D_4 \equiv c$. Then, we define $x^\Lambda = x + \Lambda_0\Theta_0 + \Lambda_1\Theta_1$, where Λ_0 and Λ_1 are Lagrange multiplier constants, and

$$\begin{aligned} x &= 4A_1C_1a^3c^3 \\ \Theta_0 &= 4(A_1^2 + C_1^2)(a^2 + c^2)^2 - 1 \\ \Theta_1 &= 4 [A_1^2a^2(a^4 + 3c^4) + C_1^2c^2(3a^4 + c^4) - 2\alpha_1]. \end{aligned} \quad (3.7)$$

Now, we want to maximize x under the constraints $\Theta_0 = \Theta_1 = 0$.

First, we solve the two constraints, whose solutions are

$$A_1^2 = \frac{8\alpha_1(u_1 + u_2) - u_2}{u_1^2 - u_2^2} \quad C_1^2 = \frac{u_1 - 8\alpha_1(u_1 + u_2)}{u_1^2 - u_2^2}, \quad (3.8)$$

where $u_1 = 4a^2(a^4 + 3c^4)$ and $u_2 = 4c^2(3a^4 + c^4)$. From $\frac{\partial x^\Lambda}{\partial A_1} = \frac{\partial x^\Lambda}{\partial C_1} = 0$ one can express the Lagrange multiplier constants as

$$\Lambda_0 = -\frac{A_1^2u_1 - C_1^2u_2}{A_1C_1} \frac{2a^3c^3}{u_1^2 - u_2^2} \quad \Lambda_1 = \frac{A_1^2 - C_1^2}{A_1C_1} \frac{2a^3c^3}{u_1 - u_2}. \quad (3.9)$$

Combining Eqs. (3.8), (3.9), and $\frac{\partial x^\Lambda}{\partial a} = \frac{\partial x^\Lambda}{\partial c} = 0$, we obtain

$$8\alpha_1(z^2 + 1)^4 = z^8 + 6z^4 + 1, \quad (3.10)$$

where $z = \frac{a}{c}$. Then, the maximum of x with given y becomes

$$x_{max} = \frac{z^3 \sqrt{8\alpha_1(1 - 8\alpha_1)(1 + z^2)^6 - z^2(3 + z^4)(1 + 3z^4)}}{(z^4 - 1)^3}. \quad (3.11)$$

Using Eq. (3.10) and performing long and tedious calculation, one can show that the right-hand side of Eq. (3.11) reduces to $\frac{1}{16} (1 - \sqrt{16\alpha_1 - 1})^2$, which results in the identical equation with Eq. (3.5). This implies that there is no one-qubit product three-qubit GHZ state in the RGHZ-symmetric states. This completes the proof.

From this theorem one can conclude that there is no $L_{0_{3\oplus\bar{1}}0_{3\oplus\bar{1}}}$ in the RGHZ-symmetric states, because this class involves one-qubit product GHZ-state. Since it is well-known that the three-qubit states consist of fully separable (S), bi-separable (B), W, and GHZ states, and they satisfy a linear hierarchy $S \subset B \subset W \subset \text{GHZ}$, theorem 2 also implies that there is no one-qubit product W state in the RGHZ-symmetric states. Thus, RGHZ symmetry excludes $L_{a_20_{3\oplus\bar{1}}}$ too because this class contains one-qubit product W state when $a = 0$. This

theorem also implies that there is no one-qubit product one-qubit product B state, which excludes $L_{a_2b_2}$. Similarly, one can exclude all classes except G_{abcd} -class⁶.

C. G_{abcd}

Now, we want to discuss the entanglement classes of remaining RGHZ-symmetric states. In order to conjecture the classes quickly, let us consider the following double bi-separable state

$$|\psi^{BB}\rangle = \frac{1}{\sqrt{2}}(|00\rangle + |11\rangle) \otimes \frac{1}{\sqrt{2}}(|00\rangle + |11\rangle). \quad (3.12)$$

Such a state belongs to G_{abcd} with $(a = 1, b = c = d = 0)$ or $a = b = c = d$. Then, Eq. (3.3) shows that the parameters of $\rho_4^{\text{GHZL}}(\psi^{BB})$ are $x = 1/8$ and $y = \sqrt{2}/8$, which correspond to the right-upper corner of the triangle in Fig. 2. Since mixing can result only in the same or a lower entanglement class, the entanglement class of this corner state should be G_{abcd} or its sub-classes. However, the sub-class of this state should be a class, where fully separable states belong, and those states are confined in $ABCD$. Therefore, the corner should be G_{abcd} . This fact strongly suggests that all remaining states in Fig. 2 are G_{abcd} . The following theorem shows that our conjecture is correct.

Theorem 3. *All remaining RGHZ-symmetric states in Fig. 2 are G_{abcd} -class.*

Proof. Let $|\psi^{BB}\rangle = (G_1 \otimes G_2 \otimes G_3 \otimes G_4)(|00\rangle + |11\rangle) \otimes (|00\rangle + |11\rangle)$, where G_j is given in Eq. (3.6). Then, it is easy to compute the parameters x and y of $\rho_4^{\text{GHZL}}(\psi^{BB})$ using Eq. (3.3). Similar to the previous theorems we want to maximize x with given y . From a symmetry of Lagrange multiplier equations it is evident that the maximum of x occurs

⁶ For other classes it is more easy to adopt the following numerical calculation than applying the Lagrange multiplier method. First, we select a representative state $|\psi\rangle$ for each SLOCC class. Next, we generate 16 random numbers and identify them with A_j, B_j, C_j, D_j ($j = 1, \dots, 4$). Then, using a mapping (3.3) one can compute x and y for pure state $G_1 \otimes G_2 \otimes G_3 \otimes G_4|\psi\rangle$. Repeating this procedure over and over and collecting all (x, y) data, one can deduce numerically the residential region of this class. Our numerical calculation shows that the residence of all SLOCC class except G_{abcd} is confined in the polygon ABCD of Fig. 2.

when

$$\begin{aligned}
A_1 = A_2 &\equiv a_1 & A_3 = A_4 &\equiv a_3 \\
B_1 = B_2 &\equiv b_1 & B_3 = B_4 &\equiv b_3 \\
C_1 = C_2 &\equiv c_1 & C_3 = C_4 &\equiv c_3 \\
D_1 = D_2 &\equiv d_1 & D_3 = D_4 &\equiv d_3.
\end{aligned} \tag{3.13}$$

For later convenience we define $\mu_1 = a_1^2 + b_1^2$, $\mu_2 = a_3^2 + b_3^2$, $\mu_3 = c_1^2 + d_1^2$, $\mu_4 = c_3^2 + d_3^2$, $\nu_1 = a_1c_1 + b_1d_1$, and $\nu_2 = a_3c_3 + b_3d_3$.

In order to apply the Lagrange multiplier method we define $x^\Lambda = x + \Lambda_0\Theta_0 + \Lambda_1\Theta_1$, where

$$\begin{aligned}
x &= \frac{1}{2} (\mu_1\mu_2\mu_3\mu_4 + \nu_1^2\nu_2^2) \\
\Theta_0 &= (\mu_1^2 + 2\nu_1^2 + \mu_3^2)(\mu_2^2 + 2\nu_2^2 + \mu_4^2) - 1 \\
\Theta_1 &= (\mu_1^2 + \mu_3^2)(\mu_2^2 + \mu_4^2) + 4\nu_1^2\nu_2^2 - 8\alpha_1.
\end{aligned} \tag{3.14}$$

The constraints $\Theta_0 = 0$ and $\Theta_1 = 0$ come from $\langle \psi^{BB} | \psi^{BB} \rangle = 1$ and Eq. (3.3), respectively.

Now, we have eight equations $\frac{\partial x^\Lambda}{\partial \mu_i} = 0$ ($i = 1, 2, 3, 4$), $\frac{\partial x^\Lambda}{\partial \nu_i} = 0$ ($i = 1, 2$), and $\Theta_0 = \Theta_1 = 0$. Analyzing those equations, one can show that the maximum of x occurs when $\mu_1 = \mu_3$ and $\mu_2 = \mu_4$. Then, the constraint $\Theta_1 = 0$ implies

$$x_{max} = \frac{1}{16} + \frac{y}{2\sqrt{2}}, \tag{3.15}$$

which corresponds to the right side of the triangle in Fig. 2. This fact implies that the whole RGHZ-symmetric states are G_{abcd} or its sub-class. Since L_{abc_2} are confined in the polygon ABCD and the remaining classes except G_{abcd} are already excluded, the states outside the polygon ABCD should be G_{abcd} -class, which completes the proof.

Although we start with a double bi-separable state, this fact does not implies that all states outside the polygon are double bi-separable because G_{abcd} contains 4-way entangled states as well as double bi-separable states. The only fact we can say is that all states outside the polygon ABCD are G_{abcd} -class.

IV. CONCLUSION

In this paper the GHZ and RGHZ symmetries in four-qubit system are examined. It is shown that the whole RGHZ-symmetric states involve only two SLOCC classes, L_{abc_2} and

G_{abcd} . Following Ref. [17] we can use our result to construct the optimal witness $\mathcal{W}_{G_{abcd}\setminus L_{abc_2}}$, which can detect the G_{abcd} -class optimally from a set of L_{abc_2} plus G_{abcd} states.

As remarked earlier if we choose GHZ symmetry, the symmetric states are represented by three real parameters as Eq. (2.1) shows. Probably, these symmetric states involve more kinds of the four-qubit SLOCC classes. The SLOCC classification of Eq. (2.1) will be explored in the future.

Another interesting extension of present paper is to generalize our analysis to any $2n$ -qubit system. Then, our modification of symmetry should be changed into ‘any one-pair, two-pair, \dots , and n -pair flips’. This would drastically reduce the number of free parameters in the set of symmetric states. This strongly restricted symmetry may shed light on the SLOCC classification of the multipartite states.

Acknowledgement: This work was supported by the Kyungnam University Foundation Grant, 2013.

-
- [1] R. Horodecki, P. Horodecki, M. Horodecki, and K. Horodecki, *Quantum Entanglement*, Rev. Mod. Phys. **81** (2009) 865 [quant-ph/0702225] and references therein.
 - [2] C. H. Bennett, G. Brassard, C. Crepeau, R. Jozsa, A. Peres and W. K. Wootters, *Teleporting an Unknown Quantum State via Dual Classical and Einstein-Podolsky-Rosen Channels*, Phys.Rev. Lett. **70** (1993) 1895.
 - [3] C. H. Bennett and S. J. Wiesner, *Communication via one- and two-particle operators on Einstein-Podolsky-Rosen states*, Phys. Rev. Lett. **69** (1992) 2881.
 - [4] V. Scarani, S. Lblisdir, N. Gisin and A. Acin, *Quantum cloning*, Rev. Mod. Phys. **77** (2005) 1225 [quant-ph/0511088] and references therein.
 - [5] A. K. Ekert, *Quantum Cryptography Based on Bells Theorem*, Phys. Rev. Lett. **67** (1991) 661.
 - [6] M. A. Nielsen and I. L. Chuang, *Quantum Computation and Quantum Information* (Cambridge University Press, Cambridge, England, 2000).
 - [7] G. Vidal, *Efficient classical simulation of slightly entangled quantum computations*, Phys. Rev. Lett. **91** (2003) 147902 [quant-ph/0301063].
 - [8] C. H. Bennett, S. Popescu, D. Rohrlich, J. A. Smolin, and A. V. Thapliyal, *Exact and asymptotic measures of multipartite pure-state entanglement*, Phys. Rev. **A 63** (2000) 012307

- [quant-ph/9908073].
- [9] G. Vidal, Entanglement monotones, *J. Mod. Opt.* **47** (2000) 355 [quant-ph/9807077].
- [10] W. Dür, G. Vidal and J. I. Cirac, *Three qubits can be entangled in two inequivalent ways*, *Phys.Rev. A* **62** (2000) 062314.
- [11] V. Coffman, J. Kundu and W. K. Wootters, *Distributed entanglement*, *Phys. Rev. A* **61** (2000) 052306 [quant-ph/9907047].
- [12] W. K. Wootters, *Entanglement of Formation of an Arbitrary State of Two Qubits*, *Phys. Rev. Lett.* **80** (1998) 2245 [quant-ph/9709029].
- [13] A. Acín, D. Bruß, M. Lewenstein, and A. Sanpera, *Classification of Mixed Three-Qubit States*, *Phys. Rev. Lett.* **87** (2001) 040401.
- [14] R. Lohmayer, A. Osterloh, J. Siewert and A. Uhlmann, *Entangled Three-Qubit States without Concurrence and Three-Tangle*, *Phys. Rev. Lett.* **97** (2006) 260502 [quant-ph/0606071]; C. Eltschka, A. Osterloh, J. Siewert and A. Uhlmann, *Three-tangle for mixtures of generalized GHZ and generalized W states*, *New J. Phys.* **10** (2008) 043014 [arXiv:0711.4477 (quant-ph)]; E. Jung, M. R. Hwang, D. K. Park and J. W. Son, *Three-tangle for Rank-3 Mixed States: Mixture of Greenberger-Horne-Zeilinger, W and flipped W states*, *Phys. Rev. A* **79** (2009) 024306 [arXiv:0810.5403 (quant-ph)]; E. Jung, D. K. Park, and J. W. Son, *Three-tangle does not properly quantify tripartite entanglement for Greenberger-Horne-Zeilinger-type state*, *Phys. Rev. A* **80** (2009) 010301(R) [arXiv:0901.2620 (quant-ph)]; E. Jung, M. R. Hwang, D. K. Park, and S. Tamaryan, *Three-Party Entanglement in Tripartite Teleportation Scheme through Noisy Channels*, *Quant. Inf. Comput.* **10** (2010) 0377 [arXiv:0904.2807 (quant-ph)].
- [15] C. Eltschka and J. Siewert, *Entanglement of Three-Qubit Greenberger-Horne-Zeilinger-Symmetric States*, *Phys. Rev. Lett.* **108** (2012) 020502 [arXiv:1304.6095 (quant-ph)].
- [16] J. Siewert and C. Eltschka, *Quantifying Tripartite Entanglement of Three-Qubit Generalized Werner States*, *Phys. Rev. Lett.* **108** (2012) 230502.
- [17] C. Eltschka and J. Siewert, *Optimal witnesses for three-qubit entanglement from Greenberger-Horne-Zeilinger symmetry*, *Quant. Inf. Comput.* **13** (2013) 0210 (2013) [arXiv:1204.5451 (quant-ph)].
- [18] C. Eltschka and J. Siewert, *Practical method to obtain a lower bound to the three-tangle*, *Phys. Rev. A* **89** (2014) 022312 [arXiv:1310.8311 (quant-ph)].
- [19] Eylee Jung and DaeKil Park, *Entanglement Classification of relaxed Greenberger-Horne-*

- Zeilinger-Symmetric States*, Quant. Inf. Comput. **14** (2014) 0937 [arXiv:1303.3712 (quant-ph)].
- [20] A. Osterloh and J. Siewert, *Entanglement monotones and maximally entangled states in multipartite qubit systems*, Quant. Inf. Comput. **4** (2006) 0531 [quant-ph/0506073].
- [21] F. Verstraete, J. Dehaene, B. De Moor, and H. Verschelde, *Four qubits can be entangled in nine different ways*, Phys. Rev. **A 65** (2002) 052112 [quant-ph/0109033].
- [22] L. Lamata, J. León, D. Salgado, and E. Solano, *Inductive entanglement of four qubits under stochastic local operations and classical communication*, Phys. Rev. **A 75** (2007) 022318 [quant-ph/0603243]; Y. Cao and A. M. Wang, *Discussion of the entanglement classification of a 4-qubit pure state*, Eur. Phys. J. **D 44** (2007) 159; O. Chterental and D. Z. Djoković, in *Linear Algebra Research Advances*, edited by G. D. Ling (Nova Science Publishers, Inc., Hauppauge, NY, 2007), Chap. 4, pp. 133-167; D. Li, X. Li, H. Huang, and X. Li, *SLOCC Classification for Nine Families of Four-Qubits*, Quant. Inf. Comput. **9** (2009) 0778 [arXiv:0712.1876 (quant-ph)]; S. J. Akhtarshenas and M. G. Ghahi, *Entangled graphs: A classification of four-qubit entanglement*, arXiv:1003.2762 (quant-ph); L. Borsten, D. Dahanayake, M. J. Duff, A. Marrani, and W. Rubens, *Four-Qubit Entanglement Classification from String Theory*, Phys. Rev. Lett. **105** (2010) 100507 [arXiv:1005.4915 (hep-th)].
- [23] F. Verstraete, J. Dehaene, and D. De Moor, *Normal forms and entanglement measures for multipartite quantum states*, Phys. Rev. **A 68** (2003) 012103 [quant-ph/0105090].